



Figures and figure supplements

The ectodomains determine ligand function in vivo and selectivity of DLL1 and DLL4 toward NOTCH1 and NOTCH2 in vitro

Lena Tveriakhina et al

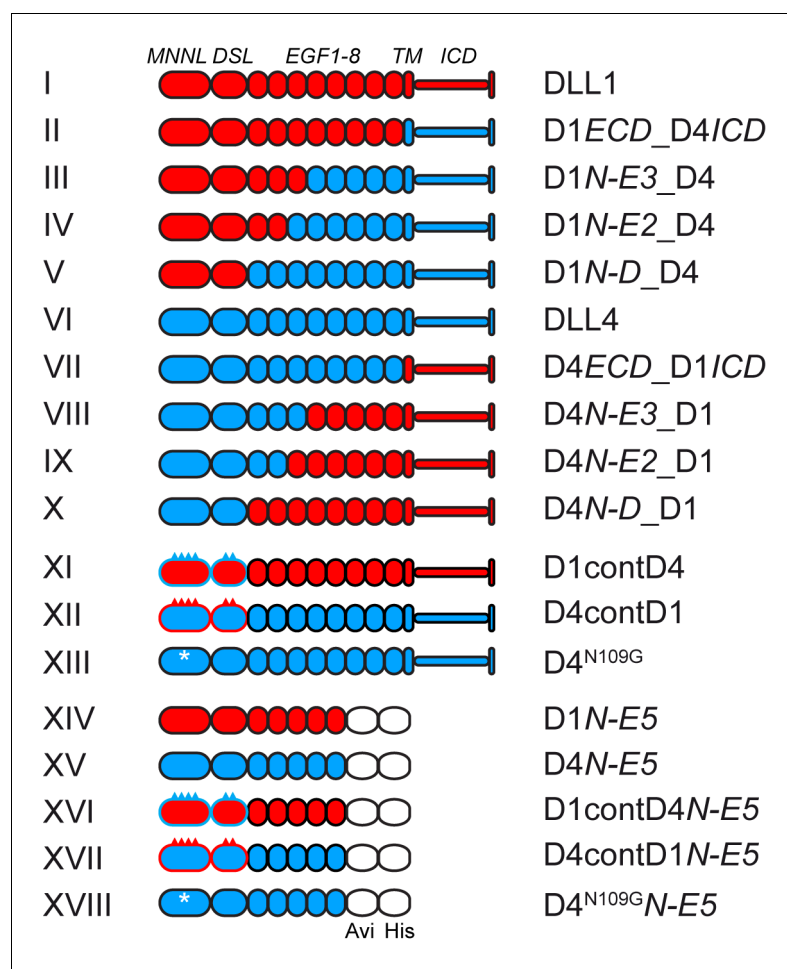


Figure 1. Schematic representation of DLL1 and DLL4 and variant proteins. I-X, full-length and chimeric ligands generated by domain swaps. XI and XII, ligands with exchanges of the known NOTCH1 contact amino acids in the MNNL and DSL domains. XIII, DLL4 variant with an N109G mutation that eliminates the N-glycosylation site in DLL4. XIV-XVIII, soluble proteins encoding the N-terminal region up to and including EGF5 carrying a C-terminal Avi-His-tag for protein purification. I-XIII were tested in cell-based Notch activation assays, II, III, VII and XI in transgenic mice, XIV-XVIII used for measurements of binding affinities to N1. Proteins analyzed in cell-based assays were C-terminally Flag-tagged, proteins analyzed in mice were untagged. Break points and surrounding amino acid sequences and point substitutions are illustrated in **Figure 1—figure supplement 1**. Red domains/spikes: DLL1; blue domains/spikes: DLL4; white asterisks: N109G mutation. ECD, extracellular domain; N, N-terminus; D, DSL domain; E, EGF repeat; TM, transmembrane domain; ICD, intracellular domain; D, DLL; cont, N1 contact amino acids.

DOI: <https://doi.org/10.7554/eLife.40045.003>

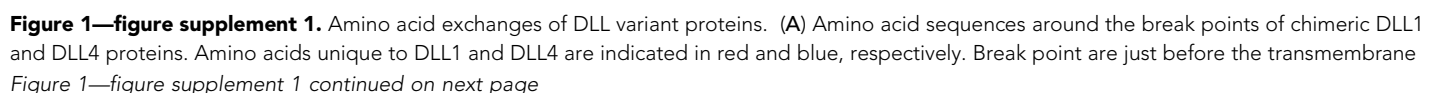


Figure 1—figure supplement 1 continued

domain (a), between EGF3 and 4 (b), EGF 2 and 3 (c), and DSL and EGF1 (d). (B) Amino acid sequences of the MNNL and DSL domains of DLL1 and DLL4 and ligand proteins with exchanges of amino acids that contact N1. N1 contact amino acids based on DLL1 and DLL4 structure alignments are depicted in black boxes. Amino acids unique to DLL1 and DLL4 are indicated in red and blue, respectively.

DOI: <https://doi.org/10.7554/eLife.40045.004>

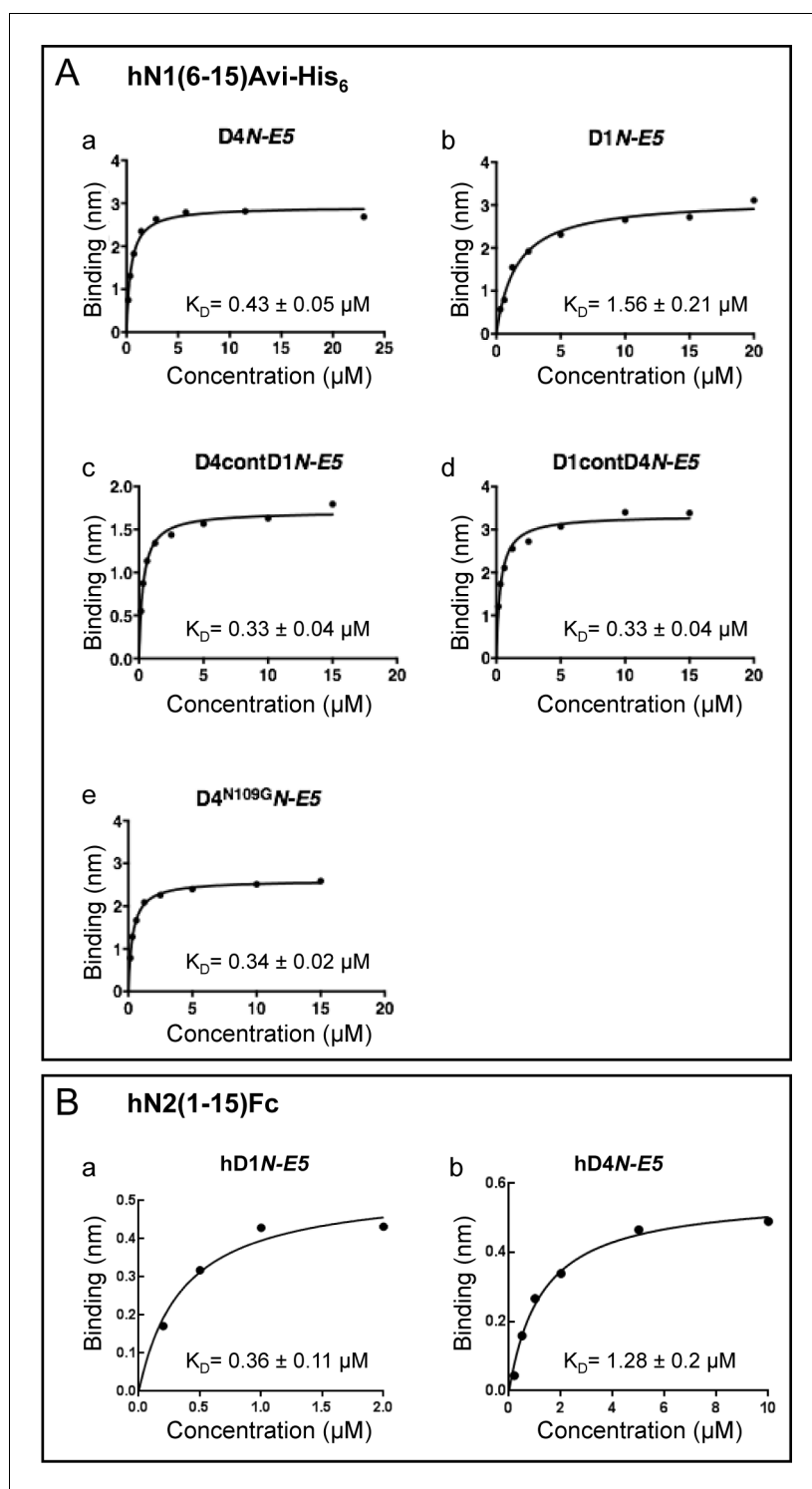


Figure 1—figure supplement 2. Analysis of ligand receptor binding. (A) Analysis of the binding of various ligands to a biotinylated human N1 ectodomain fragment containing EGF repeats 6–15 using biolayer interferometry. Binding of DLL4 (from the N-terminus through EGF-repeat 5; (a)), DLL1 (from the N-terminus through EGF-repeat 5; (b)), D4contD1 (c), D1contD4 (d), or D4^{N109G} (e) to the N1 fragment was measured after the N1 fragment was immobilized on a streptavidin sensor tip. The data were analyzed using a single-site binding model using GraphPad Prism software. Calculated K_D values and SEM are shown below the graphs. (B) Analysis of DLL1 and DLL4 binding to human N2 using biolayer interferometry. Detection of DLL1 (from the N-terminus through EGF-repeat 5; (a)) or DLL4 (from the N-terminus through EGF-repeat 5; (b)) binding to N2(1–15)-Fc

Figure 1—figure supplement 2 continued on next page

Figure 1—figure supplement 2 continued

immobilized on a protein A sensor tip. The data were analyzed using a single-site binding model using GraphPad Prism software. Calculated K_D values and SEM are shown below the graphs.

DOI: <https://doi.org/10.7554/eLife.40045.005>

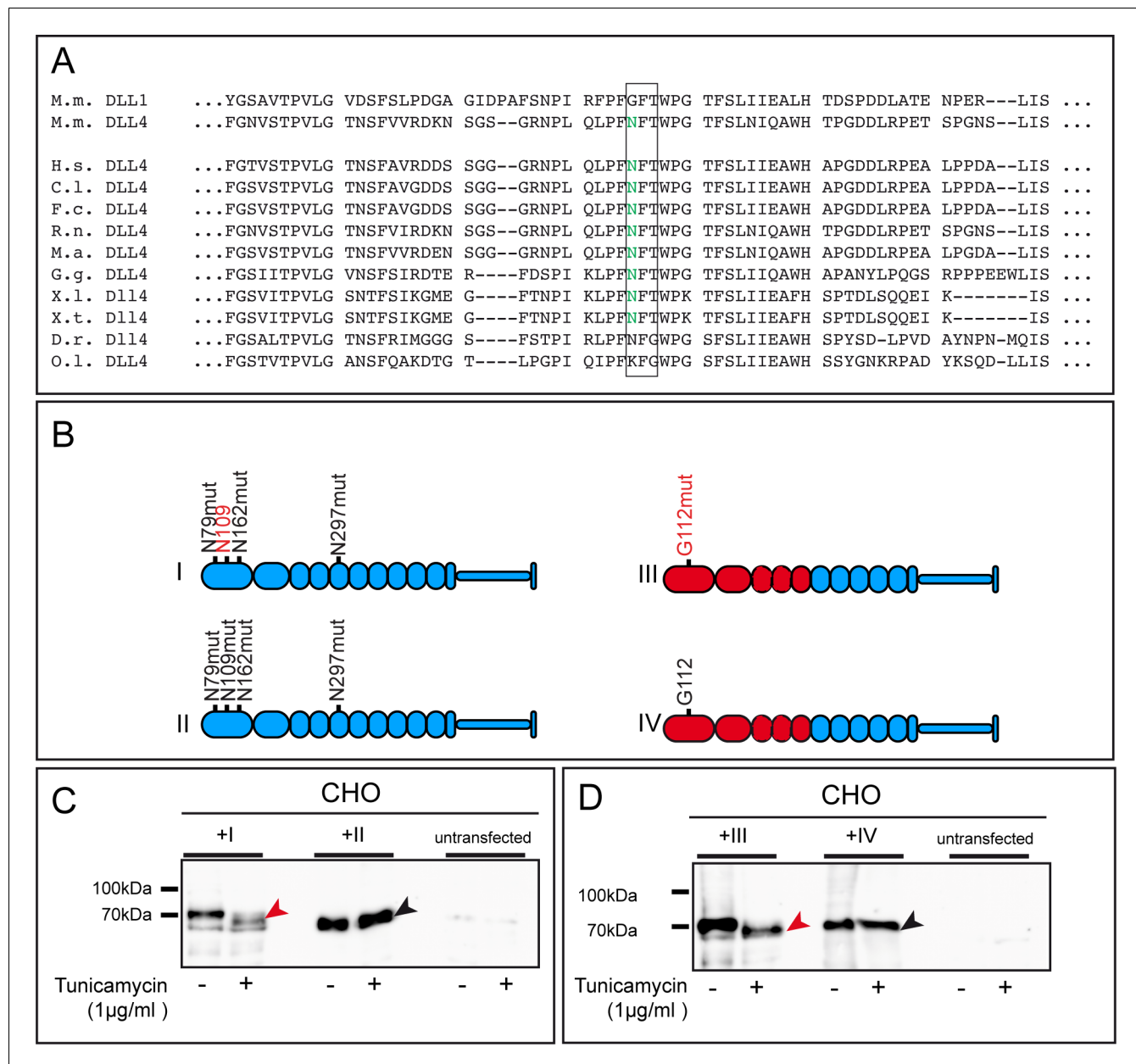


Figure 1—figure supplement 3. N109 is highly conserved and N-glycosylated in DLL4. (A) Alignment of murine DLL1 and DLL4 and of mammalian, bird, amphibian, and fish DLL4 showing the conserved N-glycosylation consensus site (green Asp in black box) in DLL4 proteins. M.m., *Mus musculus*; H.s., *Homo sapiens*; C.l., *Canis lupus* (dog); F.c., *Felis catus* (cat); R.n., *Rattus norvegicus*; M.a., *Mesocricetus auratus* (Gold hamster); G.g., *Gallus gallus* (chicken); X.l., *Xenopus leavis*; X.t., *Xenopus tropicalis* (frog); D.r., *Danio rerio* (zebrafish); O.l., *Oryzias latipes* (medaka). (B) Constructs used to validate the glycosylation state of N109 in DLL4. (I) DLL4 protein with mutated consensus sites N79, N162 and N297. (II) DLL4 protein with additionally mutated consensus site N109. The region around the N residues was exchanged from NVS to SAV (in case of N79) and from EQNDTL to LHSSGR (in case of N162) reflecting the sequence context in DLL1 lacking these consensus sites. N109 was changed to G. To prevent N-glycosylation of N297, S299 was mutated to A as found in DLL1. (III) represents a chimeric ligand with the N-terminus up to and including EGF3 of DLL1 fused to EGF4 and the C-terminal part of DLL4. Amino acid G112 was mutated to N (G112mut) generating an N-glycosylation consensus sequence like in DLL4. (IV) Chimeric ligand with the N-terminus up to and including EGF3 of DLL1 fused to EGF4 and the C-terminal part of DLL4 lacking all functional N-glycosylation sites. Red domains: DLL1; blue domains: DLL4. (C, D) CHO cells were transfected with constructs (I or II) (C) or (III or IV) (D) and treated with tunicamycin to prevent N-glycosylation. Red arrowhead in (C) points to faster migrating protein species in tunicamycin treated cells indicating N109 glycosylation. In contrast construct II did not show a shift in protein size upon treatment (black arrowhead). (D) Generation of the consensus site in the MNNL domain of DLL1 (III) resulted in N-glycosylation as tunicamycin treatment led to a shift in protein size (red arrowhead) compared to the construct with the wild type DLL1 MNNL domain (IV, black arrowhead).

DOI: <https://doi.org/10.7554/eLife.40045.006>

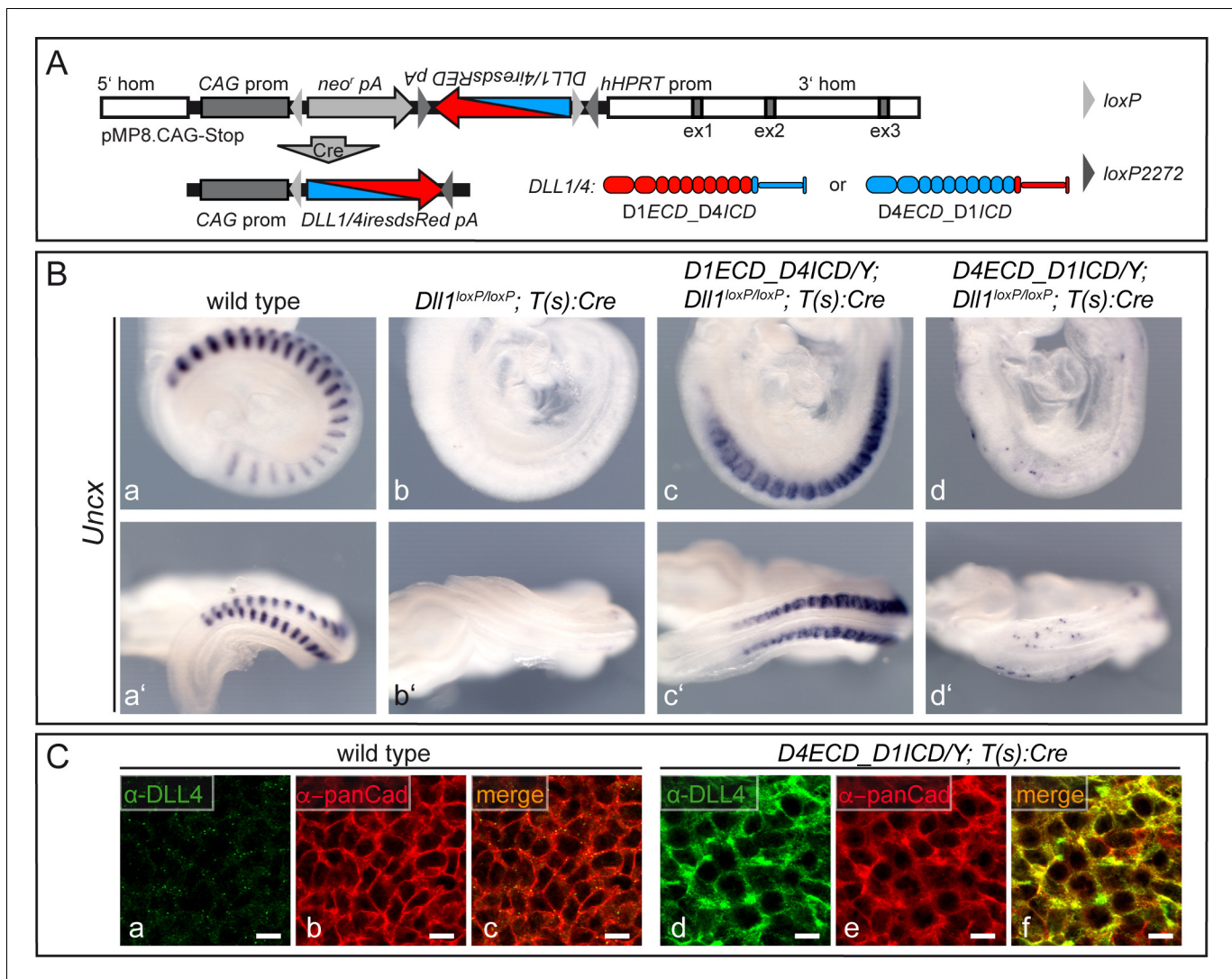


Figure 2. The extracellular domains of DLL1 and DLL4 determine ligand behavior during somitogenesis. (A) Scheme of the targeting vector pMP8. CAG-Stop used to introduce inducible chimeric ligands into the *Hprt* locus, and of Cre-mediated activation of transgene (*D1ECD_D4ICD* or *D4ECD_D1ICD*) expression driven by the CAG promoter (CAG prom). 5' hom and 3' hom, *Hprt* 5' and 3' homology regions; ex1-3 (grey boxes), *Hprt* exons; neo^r, neomycin phosphotransferase; pA, polyadenylation signal; hHPRT prom, human *Hprt* promoter; *DLL1/4iresdsRed*, chimeric ORF-linked to dsRed tag by an internal ribosomal entry site (IRES). (B) *Uncx* expression in E9.5 wild type embryos (a, a'; n = 28), embryos lacking DLL1 in the mesoderm (b, b'; n = 12) and male embryos lacking DLL1 in the mesoderm that express either *D1ECD_D4ICD* (c, c'; n = 9) or *D4ECD_D1ICD* (d, d'; n = 8) showing that the extracellular domain of DLL1 but not of DLL4 can restore *Uncx* expression. (C) Whole mount immunofluorescent staining of wild type (a–c) and *D4ECD_D1ICD*/*Y*;T(s):Cre (d–f) PSMs using antibodies recognizing the extracellular domain of DLL4 showing co-localization of the exogenous chimeric ligand with pan-Cadherin (panCad) at the cell surface. Additional intracellular staining most likely reflects the presence of the ligand in the ER and trans Golgi as observed previously for DLL1 in cultured cells (Geffers et al., 2007; Müller et al., 2014) and for endogenous DLL1 and transgenic DLL4 in the PSM (Preuß et al., 2015). n = 3 for wild type, n = 4 for *D4ECD_D1ICD*/*Y*;T(s):Cre; Scale bar = 10 μ m.

DOI: <https://doi.org/10.7554/eLife.40045.007>

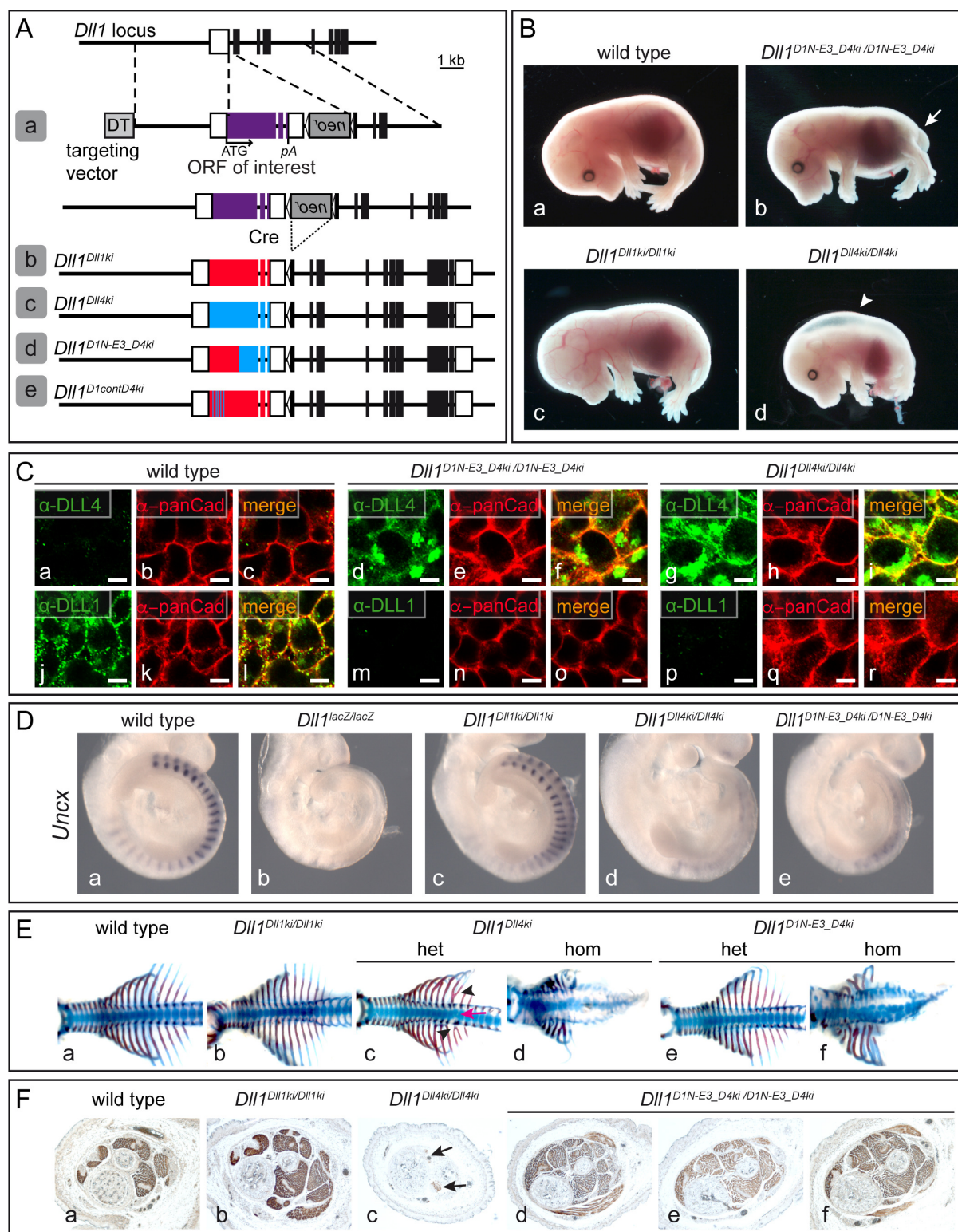


Figure 3. D1N-E3_D4 is not able to compensate for DLL1 function during somitogenesis. (A) "Mini-gene" targeting strategy to express DLL1 or DLL4 variants from the *Dll1* locus (a) and alleles generated in this study (d and e). The *Dll1^{Dll1ki}* (b) and *Dll1^{Dll4ki}* (c) control alleles were described previously Figure 3 continued on next page

Figure 3 continued

(Preuße et al., 2015; Schuster-Gossler et al., 2016). *Dll1*^{D1N-E3_D4ki} (d) encodes a fusion protein between the N-terminal part of DLL1 including EGF3 fused to EGF4 and the remaining C-terminal portion of DLL4 (III in **Figure 1** and **Figure 1—figure supplement 1Ab**). *Dll1*^{D1contD4ki} (e) encodes a DLL1 variant whose predicted amino acids of the MNBL and DSL domains that contact N1 are replaced by the corresponding amino acids of DLL4 (XI in **Figure 1**, **Figure 5C**, and **Figure 1—figure supplement 1B**). All alleles have an identical structure and intron 9 and 10 sequences of *Dll1*. (B) External phenotypes of wild type (a; n = 19), homozygous *Dll1*^{D1N-E3_D4ki} (b; n = 11), *Dll1*^{Dll1ki} (c; n = 3) and *Dll1*^{Dll4ki} (d; n = 3) control E15.5 fetuses. Arrow in (b) points to the short tail. Arrowhead in (c) points to edemas present in homozygous *Dll1*^{Dll4ki} fetuses. (C) Indirect immunofluorescence staining of wild type (a–c, j–l), homozygous *Dll1*^{D1N-E3_D4ki} (d–f, m–o), and homozygous *Dll1*^{Dll4ki} (g–i, p–r) E9.5 PSMs using antibodies recognizing the extracellular domain of DLL4 (a, d, g) and DLL1 (j, m, p) and pan-Cadherin (panCad; b, e, h, k, n, q) showing expression of D1N-E3_D4 and co-localization with the cell surface marker pan-Cadherin. Staining of D1N-E3_D4 appears weaker than DLL4 most likely because much of the epitope recognized by the polyclonal anti-DLL4 antibody is missing in this chimeric protein. n ≥ 3; Scale bar = 5 μm. (D) WISH of E9.5 embryos showing that D1N-E3_D4 does not restore normal *Uncx* expression (e; n = 10) resembling the *Dll1*^{Dll4ki} phenotype (d; n = 7). (E) Skeletal preparations of wild type (a; n = 11), homozygous *Dll1*^{Dll1ki} (b; n = 6), heterozygous (c; n = 14/16) and homozygous (d; n = 3) *Dll1*^{Dll4ki}, and heterozygous (e; n = 14) and homozygous (f; n = 10) *Dll1*^{D1N-E3_D4ki} E15.5 fetuses. Arrow and arrowheads in (c) point to axial skeleton defects that were not detected in *Dll1*^{D1N-E3_D4ki} heterozygotes (e). (F) Cross-sections of hind limbs of wild type (a), homozygous *Dll1*^{Dll1ki} (b), homozygous *Dll1*^{Dll4ki} (c), and homozygous (d–f; n = 3) *Dll1*^{D1N-E3_D4ki} E18.5 fetuses stained for expression of Myosin Heavy Chain (MHC) indicating that D1N-E3_D4 rescues the skeletal muscle phenotype in contrast to DLL4. Arrows in (c) point to skeletal muscle remnants.

DOI: <https://doi.org/10.7554/eLife.40045.008>

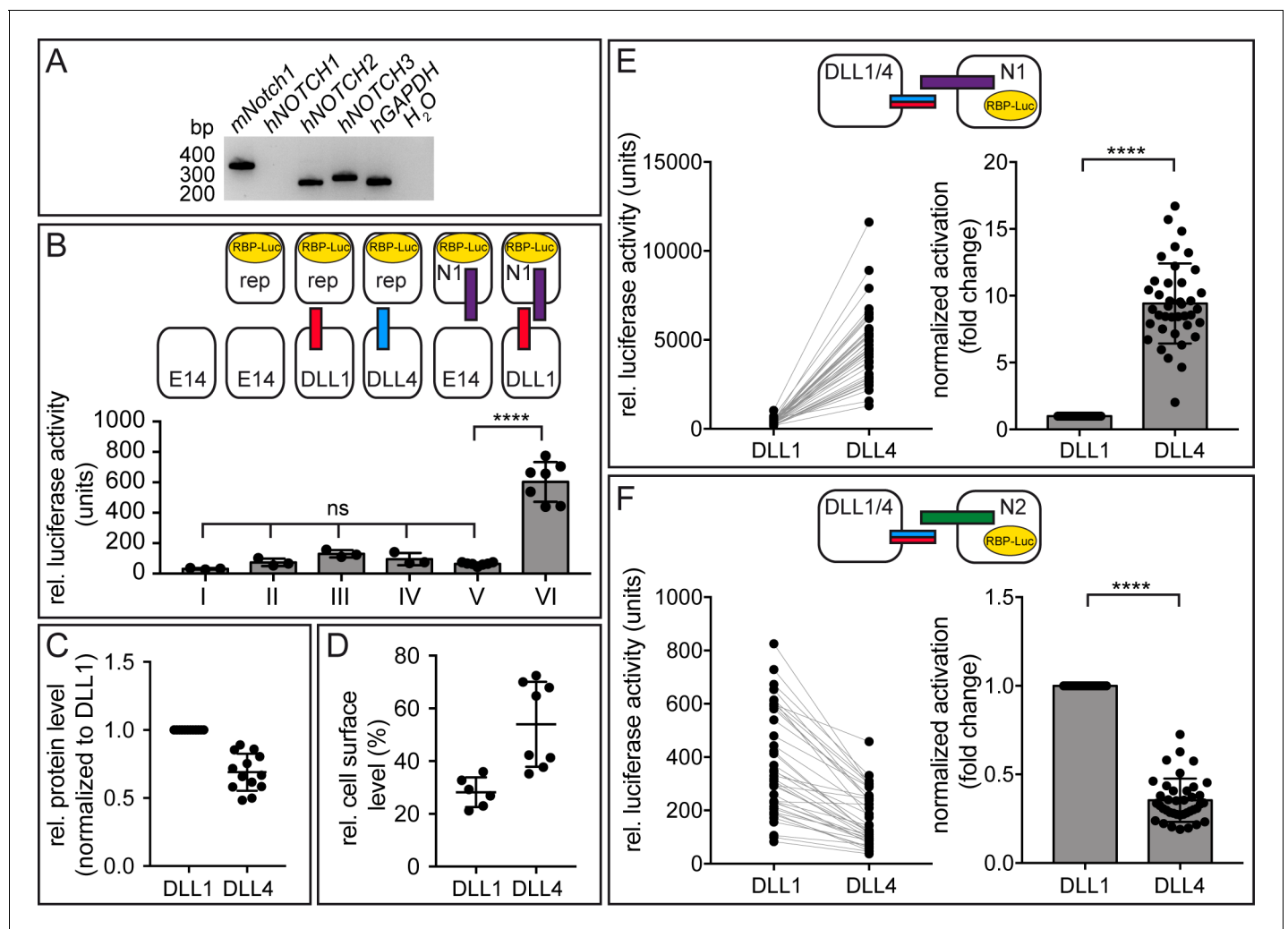


Figure 4. DLL1 and DLL4 differentially activate NOTCH1 and NOTCH2 in cell-based co-culture assays. (A) RT-PCR analysis using RNA of HeLaN1 cells shows the expression of endogenous human *NOTCH2* and *NOTCH3* in addition to the exogenous murine *Notch1*. (B) ES cell-based trans-activation assays demonstrate that E14TG2a ES cells express negligible amounts of endogenous Notch receptors and ligands. Co-cultivation of ES cells with stable expression of either DLL1 (III) or DLL4 (IV) from the *Hprt*-locus with ES-cells carrying only the RBP-Luc reporter in the *Hprt*-locus (E14rep) showed luciferase activity at levels indistinguishable from lysates of only E14 cells (I) and co-cultures of wild type E14 and reporter carrying ES cells (II). Similarly, co-culture of ES cells carrying N1 and the RBP-Luc reporter (N1rep) with E14 cells (V) did not show reporter activation significantly above background levels, whereas co-culture of DLL1 expressing cells with N1rep ES cells showed a 6–10-fold increase in luciferase activity (VI). $n \geq 3$ co-cultures with 2–4 replicate measurements per n (Figure 4—source data 1). Mean \pm SD, ns = $p \geq 0.05$, ****= $p < 0.0001$, one-way ANOVA followed by Tukey's multiple comparison test. (C) Protein expression analysis indicating similar expression levels of DLL1 and DLL4 in the ES cell clones used. Each DLL4 value represents a technical replicate, which was referenced to its paired DLL1 value, which was arbitrarily set to one for each measurement. The non-normalized values (DLL/ β -Tub ratios) are depicted in a graph in Figure 4—figure supplement 1A (Figure 4—source data 2). (D) Cell-surface biotinylation demonstrating that a slightly higher fraction of DLL4 is present at the cell surface compared to DLL1 ($n \geq 6$; Figure 4—source data 3). (E) DLL4 activates N1 about 10-fold more strongly than DLL1 in co-culture assays. Left graph shows non-normalized N1 activation. Lines connect values measured in the same assay. Right graph shows values normalized to DLL1 activation, and corrected for protein expression and cell surface presentation. (F) DLL4 activates N2 about half as strongly as does DLL1. Left graph shows non-normalized N2 activation. Lines connect values measured in the same assay. Right graph shows values normalized to DLL1 activation, and corrected for protein expression and cell surface presentation. Each dot represents a technical replicate. Raw data are shown in Figure 4—source data 4 and Figure 4—source data 5. Co-cultures ($n = 39$) with two replicate measurements per n. Mean \pm SD, ns = $p \geq 0.05$, ****= $p < 0.0001$, Student's paired t-test.

DOI: <https://doi.org/10.7554/eLife.40045.009>

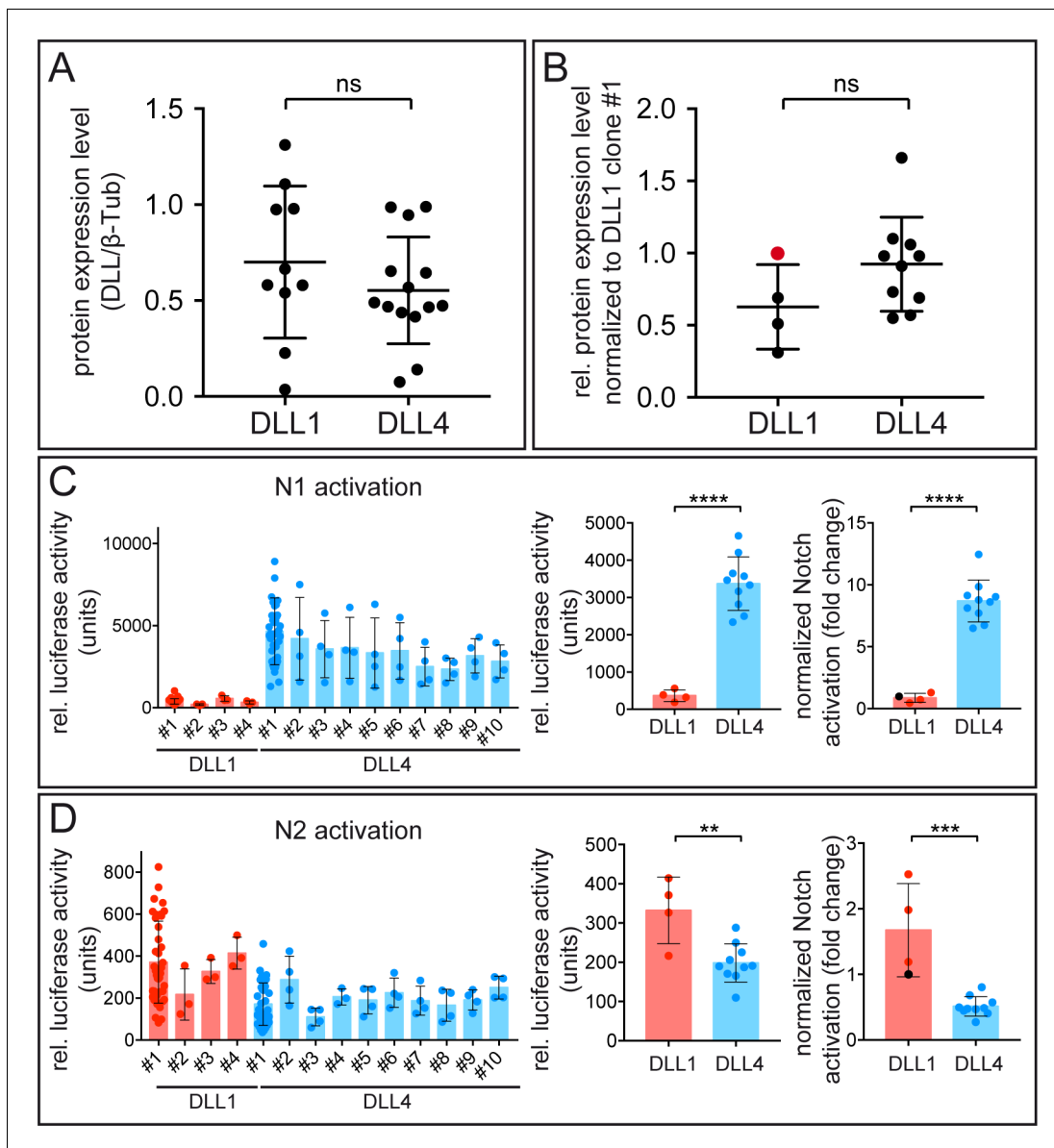


Figure 4—figure supplement 1. Consistent N1 and N2 activation by different cell clones expressing DLL4. (A) Protein expression level in DLL1 clone #1 and DLL4 clone #1 (DLL ligand/β-Tub) determined by quantitative Western blot analysis. Each dot represents a technical replicate (numerical values in **Figure 4—source data 2**). (B) Relative protein expression level in 4 and 10 independent ES cell clones, respectively, expressing DLL1 or DLL4 from the *Hprt* locus normalized to DLL1 clone #1 level measured in the same assay. Each dot represents the mean value of $n \geq 3$ independent measurements of a single clone. Red dot indicates DLL1 clone #1 that was used for normalization. For numerical values see **Figure 4—figure supplement 1—Source Data 1**. (C) and (D) N1 and N2 activation by 4 DLL1 and 10 DLL4 expressing independent ES cell clones. Left graphs show rel. luciferase activity measured for each DLL1 and DLL4 expressing clone. Each dot represents a technical replicate of a given cell clone. Central graphs show averaged rel. luciferase activity for DLL1 and DLL4 expressing cell clones. Each dot represents the mean value of $n \geq 3$ measurements of a given cell clone. Right graphs show Notch activation normalized to activation by DLL1 clone #1 ($n \geq 3$). Black dots indicate DLL1 clone #1. For numerical values see **Figure 4—figure supplement 1—Source Data 2**. Student's unpaired t-test; Mean \pm SD, ns = not significant; **= $p \leq 0.01$; ***= $p \leq 0.001$; ****= $p \leq 0.0001$.

DOI: <https://doi.org/10.7554/eLife.40045.010>

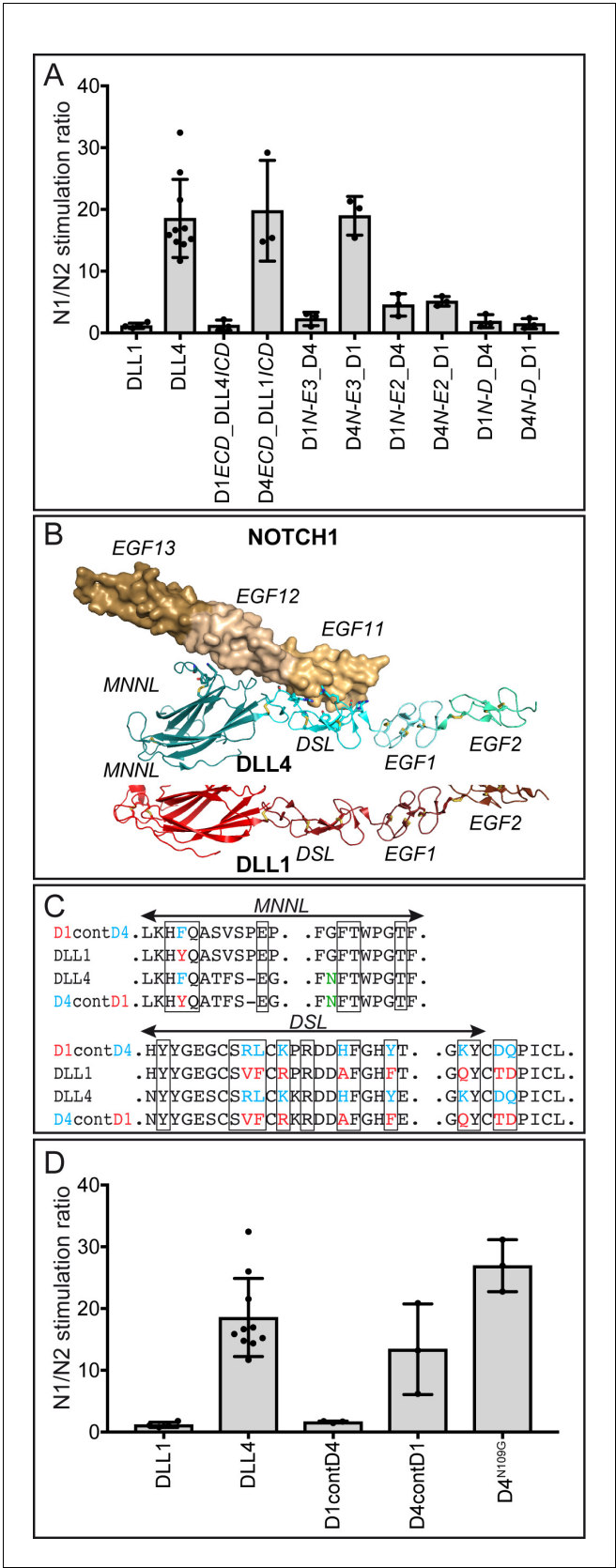


Figure 5. Contributions of the MNNL-EGF3 portion and contact amino acids to ligand selectivity towards N1 and N2. (A) N1/N2 activation ratios by DLL1 and DLL4 chimeric proteins show that receptor selectivity of DLL1 and
Figure 5 continued on next page

Figure 5 continued

DLL4 is encoded by the extracellular domain and that EGF3 contributes to N1/N2 selectivity. DLL4, D4ECD_D1/CD, and D4N-E3_D1 show N1/N2 induction ratios of ~20. DLL1, D1ECD_D4/CD, and D1N-E3_D4 exhibit induction ratios of 1–3. Chimeric pairs with domain exchanges between EGF2 and EGF3 or between DSL domain and EGF1 show equivalent stimulation ratios. Each dot represents the mean of N1 (relative luciferase units; **Figure 5—source data 1**)/N2 (relative luciferase units; **Figure 5—source data 2**) of $n \geq 3$ measurements per clone of a given ligand construct. Bars represent the Mean \pm SD of $n \geq 3$ clones per construct (**Figure 5—source data 3**). (B) Structure-based superposition of DLL1 and DLL4 (PDB ID codes 4XBM and 4XLW, respectively; (Kershaw et al., 2015; Luca et al., 2015). Top panel: NOTCH1 is rendered as a molecular surface (wheat), and DLL4 is rendered in ribbon representation (cyan). N1 contact residues on DLL4 were rendered as sticks, and were used to predict N1 contact amino acids of the MNNL and DSL domains of DLL1 (red). Domains are labeled above and below the structures, respectively, and individual domains are identified by different degrees of color shading/intensity. (C) Parts of the MNNL and DSL sequences showing the contact amino acids (boxed), the divergent amino acids of DLL1 (red) and DLL4 (blue), and the sequence of ligands with amino acid exchanges (complete sequences of the changed MNNL and DSL domains are shown in **Figure 1—figure supplement 1B**). The N-glycosylation site at residue N109 of DLL4 is indicated in green. (D) N1/N2 activation ratios of ligands with exchanged N1 contact amino acids. D1contD4 does not show changes in receptor selectivity compared to DLL1. Replacing the contact residues of DLL4 with those of DLL1 only reduces N1/N2 activation ratio to ~13. Elimination of the N-glycosylation site of DLL4 with the N109G mutation (the corresponding amino acid of DLL1) does not change DLL4 receptor selectivity. Each dot represents the mean of N1 (relative luciferase units; **Figure 5—source data 1**)/N2 (relative luciferase units; **Figure 5—source data 2**) of $n \geq 3$ measurements per clone of a given ligand construct. Bars represent the Mean \pm SD of $n \geq 3$ clones per construct (**Figure 5—source data 3**).

DOI: <https://doi.org/10.7554/eLife.40045.018>

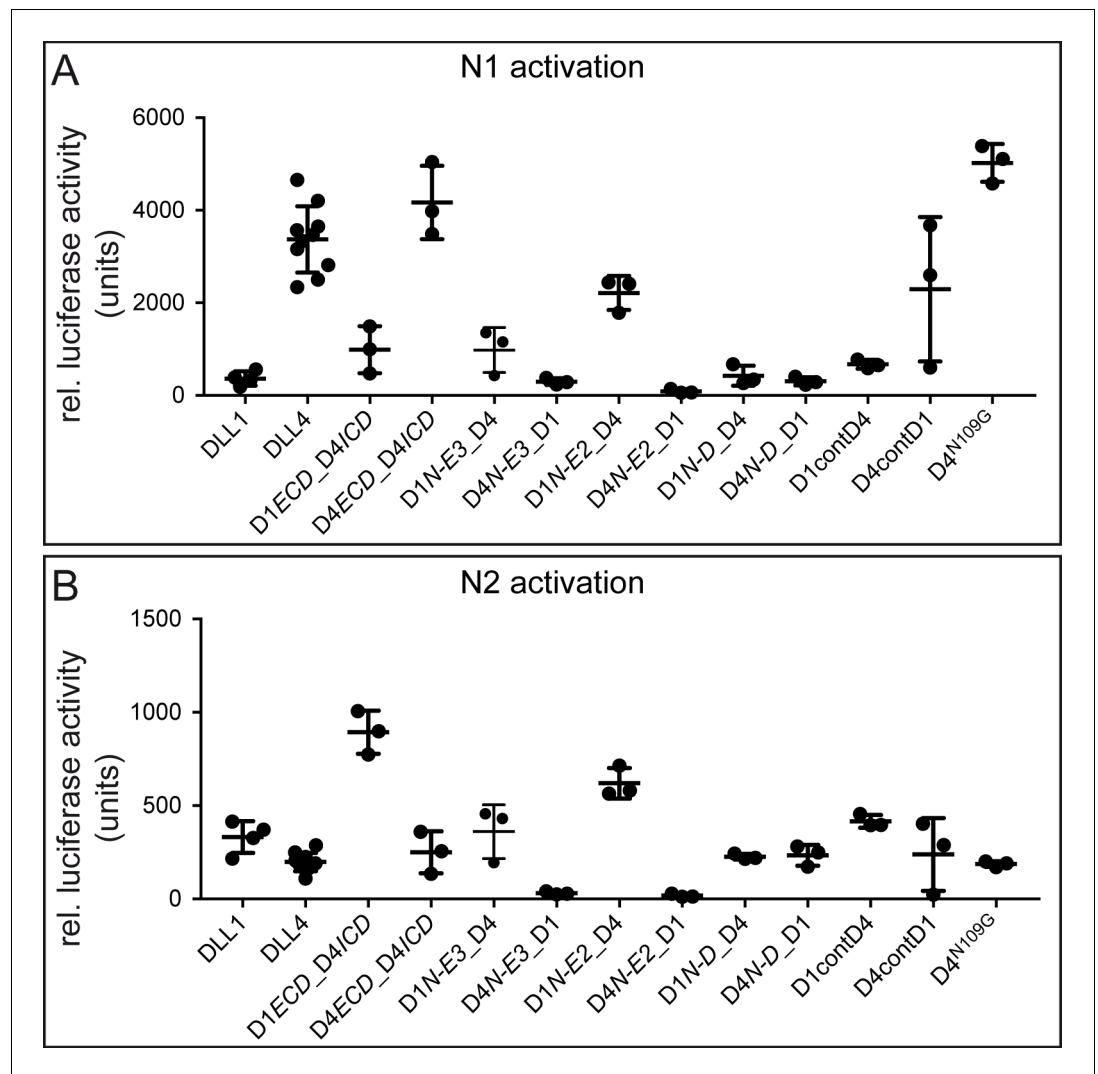


Figure 5—figure supplement 1. N1 and N2 activation by different ligand proteins. (A) and (B) Rel. luciferase activity obtained in co-cultures of ES cells expressing wild type ligands, chimeric ligands, and ligands with amino acid substitutions in the direct ligand-receptor binding region. Each dot represents the mean of $n \geq 3$ technical replicates of a given cell clone. For numerical values see **Figure 5—source datas 1** and **2**. Mean \pm SD.

DOI: <https://doi.org/10.7554/eLife.40045.019>

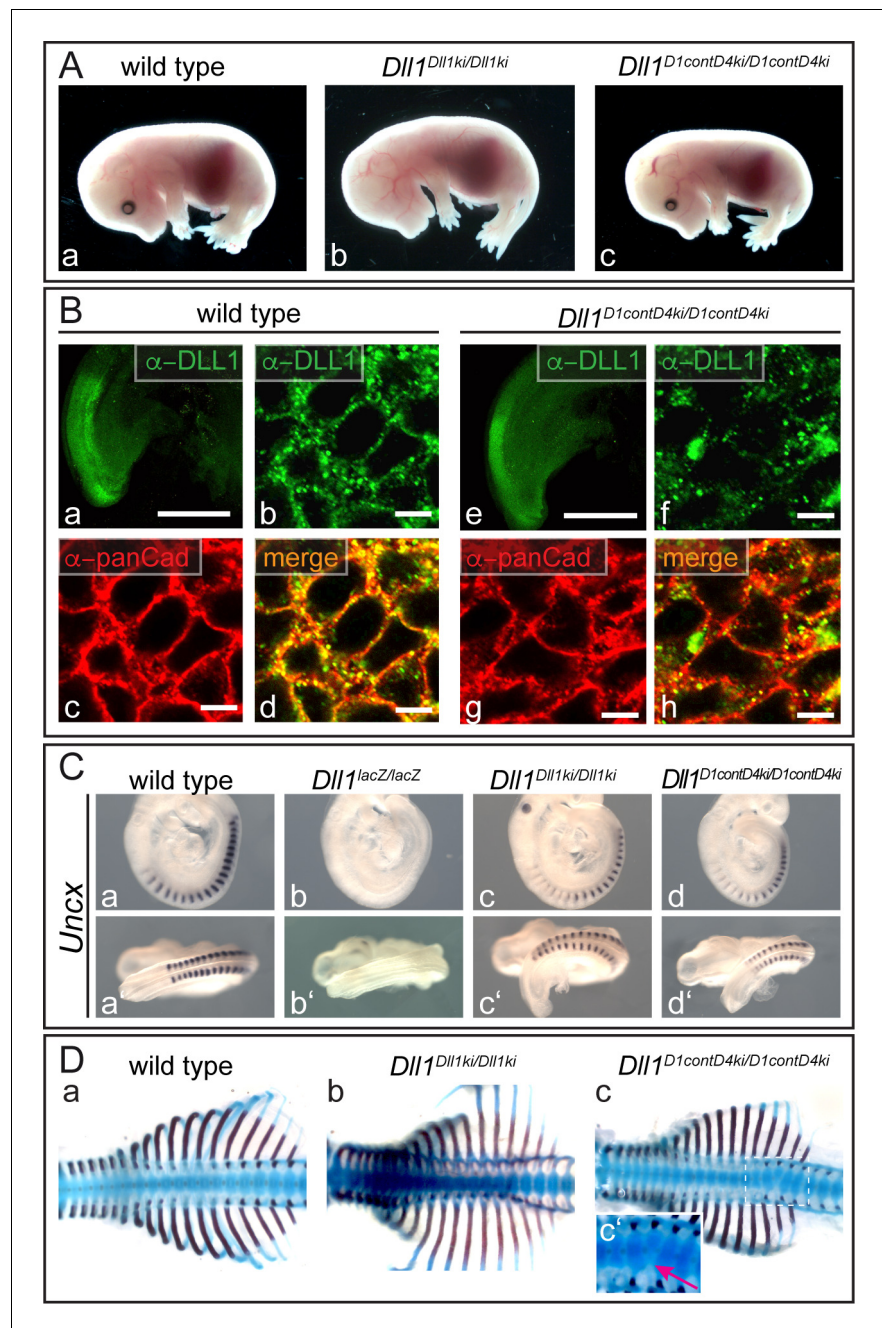


Figure 6. DLL1 carrying the DLL4 contact amino acids in the MNNL and DSL domains is a functional DLL1 ligand in vivo. (A) E15.5 *Dll1*^{D1contD4ki/D1contD4ki} (c; n = 12) fetuses are indistinguishable from wild type (a; n = 19) and *Dll1*^{Dll1^{ki}/Dll1^{ki} (b; n = 3) controls. (B) D1contD4 co-localizes with pan-Cadherin (panCad) at the cell surface of *Dll1*^{D1contD4ki/D1contD4ki} PSM cells (e-h; n ≥ 3); Scale bars: a, e = 500 μm; b-d, f-h = 5 μm. (C) Whole mount in situ hybridization showing that D1contD4 induces normal *Uncx* expression during somitogenesis (d,d'; n ≥ 5). (D) Skeletal preparations of *Dll1*^{D1contD4ki/D1contD4ki} E15.5 fetuses showing minor defects of single vertebrae in the lower thoracic region (c,c'; n = 3/4).}

DOI: <https://doi.org/10.7554/eLife.40045.023>